5-2022

Investigating the Impact of Hypoxia on Reactive Oxygen Species Generation within Murine Breast Cancer Cells

Jared McPeake

Investigating the Impact of Hypoxia on Reactive Oxygen Species Generation within Murine Breast Cancer Cells

By

Jared McPeake

Faculty Mentor: Narasimhan Rajaram

Spring 2022

Department of Biomedical Engineering

College of Engineering

University of Arkansas

Introduction

One of the most lethal aspects of cancer is its ability to migrate from a primary tumor site to almost any other location in the body through the bloodstream or lymphatic system in a process called metastasis. A study done by Fidler in 2003 showed about 90% of fatal cancers metastasize, underscoring the importance of early metastatic-potential detection within tumors[1]. Understanding the environmental factors and signaling molecules that lead to metastasis could provide an answer as to what causes the metabolic shift within the tumor that enables it to metastasize. One of the main contributors responsible for this metabolic shift to a more aggressive, metastatic state is a transcription factor known as hypoxia-inducible factor (HIF-1), a protein highly influenced by the presence of reactive oxygen species (ROS).

Reactive Oxygen Species

During respiration, oxygen serves to take up electrons exiting the electron transport chain and form water. During this reduction of oxygen gas into water, many of the partial intermediates are kept within Complex IV[2]. However, occasionally an electron may leak from another location along the electron transport chain, causing oxygen gas to spontaneously reduce to superoxide. Superoxide is a precursor to many ROS, including hydrogen peroxide and hydroxyl radical[3,4]. These highly oxidative chemicals can be damaging to nearly any molecular structure. ROS can exit the mitochondria into the cytosol via voltage-dependent anion channels [2,5]. If ROS penetrate the nucleus of the cell, DNA may be damaged, leading to mutations. To prevent this from happening, cells have ROS scavenging mechanisms using enzymes, such as catalase, reduced glutathione, and other molecules with antioxidant properties.

ROS have been heavily implicated in the endothelial to mesenchymal transition (EMT), a process in which cancer stem cells (CSCs) transition into a more metastatic phenotype, as well as field cancerization[6]. In numerous studies, ROS were found to activate various pathways, such as the Notch signaling and TAK1 pathways [6,7]. In other studies, ROS have also been shown to maintain CSCs via the NF-κB pathway, in turn causing resistance to chemotherapy and radiotherapy[6,8]. Chronic exposure to high concentrations of H_2O_2 has been shown to promote the malignant transformation of fibroblasts and epithelial cells, pointing to the formation of a pre-malignant field [9–11].

When rate of ROS scavenging is out of equilibrium with the rate of ROS production, this results in a state known as oxidative stress. The main biochemical pathway involved in the detection of oxidative stress within normal cells, and the promotion of metastasis within cancer cells, is the HIF-1 pathway.

The HIF-1 Pathway

HIF-1 is divided into two subunits: HIF-1α and HIF-1β. The HIF-1β subunit functions as a constitutively expressed aryl hydrocarbon receptor nuclear translocator, but the HIF-1α subunit functions as a hypoxia-signaling transcription factor[12,13]. Upstream from HIF-1α, prolyl hydroxylase domain (PHD) enzymes catalyze the binding of the Von Hippel (VHL) complex to HIF-1α under normoxic conditions, marking HIF-1α for ubiquitination. Under hypoxic conditions, the VHL complex is unable to bind to HIF-1α due to the absence of oxygen-containing hydroxyl groups, resulting in the accumulation of HIF-1α. Sufficient accumulation of HIF-1α in the cytosol allow it to penetrate the nucleus, binding to the HIF-1β subunit and forming HIF-1. The HIF-1 transcription factor then binds to hypoxia response elements (HREs) in the DNA[12,13].

This binding of HIF-1 to the HREs leads to upregulation of HIF-1 activated proteins such as vascular endothelial growth factor (VEGF), which encourage angiogenesis, initiate a switch to anaerobic metabolism, and other effects that lead to increased survivability and motility (Fig. 1)[12,14].

Because oxygen accepts electrons when they exit the electron transport chain, a lack of oxygen within the mitochondria results in increased generation of ROS at Complex III. When cells lacking Complex III are in a 1.5% O2 environment, HIF-1α expression is significantly attenuated, indicating that the ROS produced at Complex III are both required and sufficient for HIF-1α stabilization[15]. When ROS generation increases because of hypoxia, HIF-1α expression also increases. With increased HIF-1α expression, HIF-1α helps to counteract ROS-induced cell death by decreasing ROS levels within the cell. This same mechanism also enables cells with high levels of HIF-1α expression to be radiation-resistant[16].

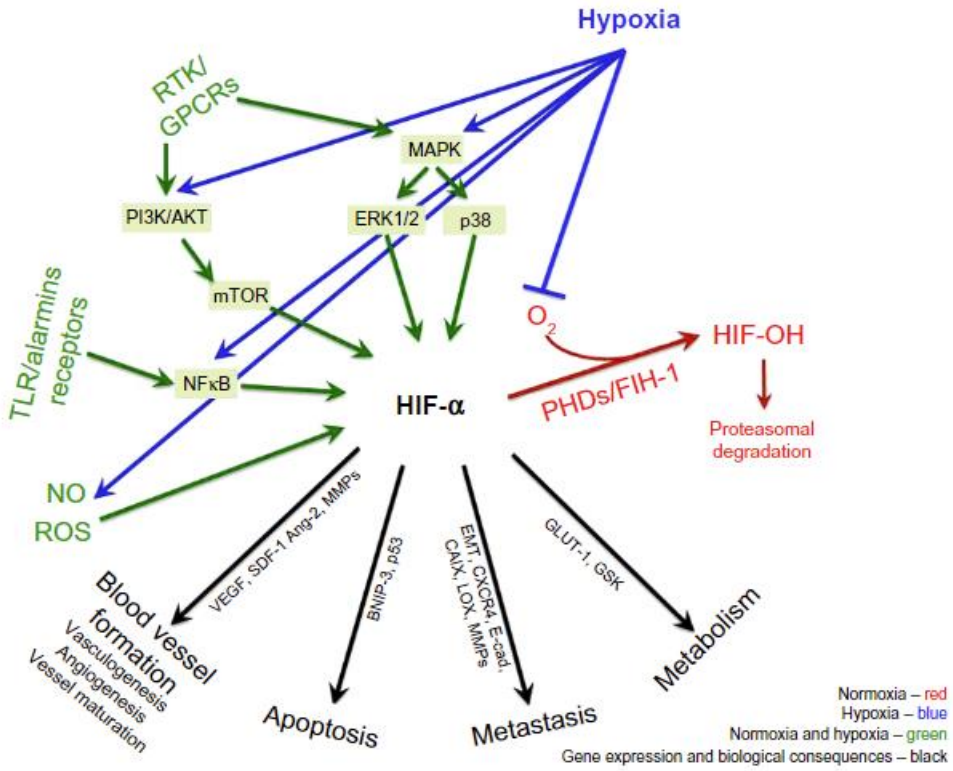

Figure 1. Molecular pathway chart displaying effects of normoxia (red lines), hypoxia (blue lines), normoxia and hypoxia (green lines) on HIF-1α, as well as downstream effects from HIF-1α. One pathway of particular interest in this study is the path leading from hypoxia to nitric oxide (NO)/reactive oxygen species (ROS), and from ROS to the stabilization of HIF-1α. Additionally, the inhibitory normoxia pathway shows how HIF-1α is degraded in the presence of oxygen. (IMG: Muz)

Defining Hypoxia and Normoxia

As shown in Figure 2, tumor oxygenation state is a function of supply and demand. On the supply side of the equation, oxidative stress can be brought about when the vasculature forms shunt flows around the tumor, contains low pO2, is not dense, or is arranged haphazardly[17]. On the demand side of the equation, tumors often undergo stages of rapid proliferation during development. As a result of this rapid proliferation of cells within the tumor, some cells experience brief periods of time in which the concentration of oxygen within the tumor microenvironment is lower than normal due to the imbalance of oxygen consumption and oxygen supply[17,18]. During this

period of imbalance, the tumor often undergoes two forms of hypoxia simultaneously due to the distance of diffusion for cells further from blood vessels and the variations in red blood cell flux through the microvessels[18]. Intermittent hypoxia, or high frequency hypoxia, occurs over short periods of time, each hypoxic period lasting about 15-20 minutes[19]. Chronic hypoxia lasts for longer periods of time, with periods lasting anywhere from hours to days. A popular analogy used to describe the relationship of these two types of hypoxia is the relationship between tides and waves in an ocean[17]. Since it may be difficult to critically examine the effects both types of hypoxia have on the HIF-1α pathway *in vivo*, there is a need to examine both forms of hypoxia on a cellular level under controlled oxygenation conditions.

Traditionally, a hypoxic environment is defined as one in which the concentration of oxygen is low enough to induce oxidative stress within cells. However, this definition becomes more complex when attempting to emulate physiological hypoxia in-vitro. When attempting to emulate the oxidative environment of a specific organ, it is important to consider the oxidative characteristics of that organ. For example, liver and kidney tissue display pronounced physiological O2 gradients that have been visualized using VEGF (downstream product of HIF-1)[20,21]. Under in-vitro conditions, it is essential that as much as possible is done to ensure that pericellular O2 levels are as close to the desired O2 levels as possible. Since the oxygen diffusion limit is only about 100-200 µm, the depth of media within a cell plate should be minimized [20,22–24]. Some strategies for verifying pericellular O2 levels include using phosphorescent dyes or gas-permeable plates. However, these methods do have their drawbacks. For example, many adherent cells do not adhere well to gas-permeable plates [20].

The definition of normoxia is also one that can vary by context. Early in hypoxia research, many researchers considered the concentration of oxygen in the air humans breathe (also known as “headspace” air), which is 21% O2, to be normoxic. However, upon additional consideration, the definition of normoxia has evolved to take the physiological conditions of the tumor microenvironment into account [20]. When examining the efficiency at which the alveoli of the lungs convert atmospheric oxygen into blood oxygen, it becomes obvious that this 21% number is much closer to hyperoxic levels than normoxic level[20]. The oxygenation status of different tissues in the body is not thoroughly defined, but some studies state a median O2% of 6.8-8.5% within tissue surrounding breast cancer tumors[14,25,26].

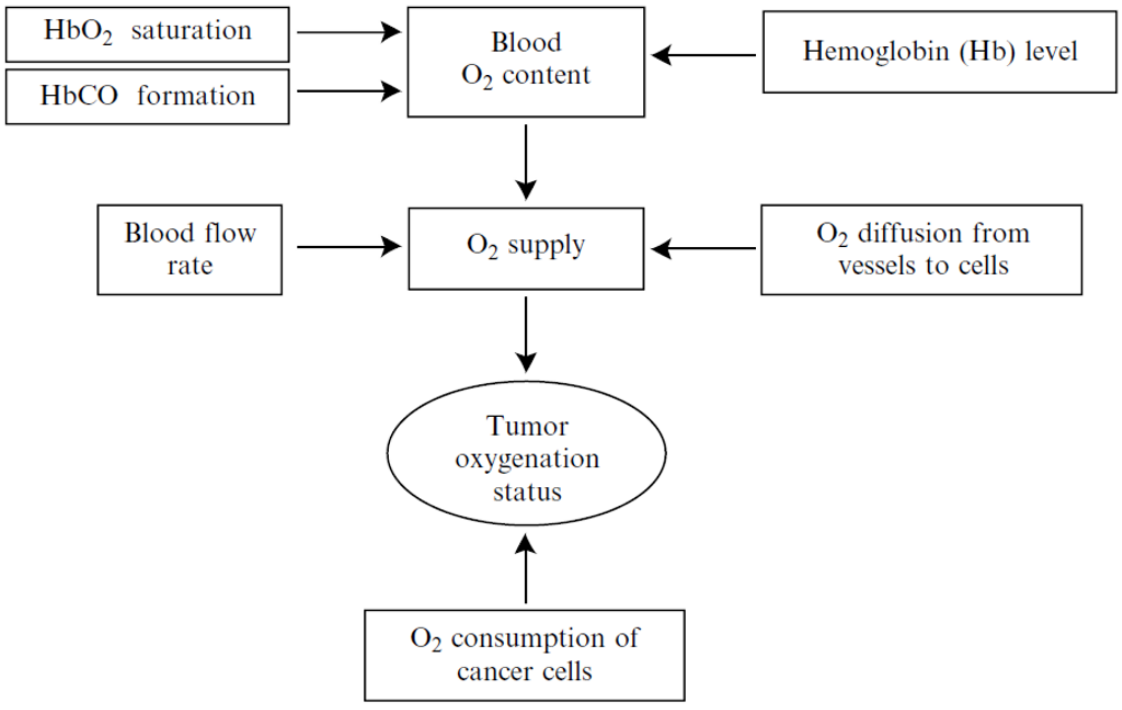

Figure 2. Flowchart depicting causes of hypoxia in-vivo. The top half of the figure shows various factors that impact oxygen supply to the tumor. The bottom half shows that O2 consumption can also impact the overall oxygenation state of the tumor. (IMG: Vaupel)

Interaction Between Hypoxia, Metabolism, and Metastasis

Perhaps at risk of oversimplification, the interaction between hypoxia, metabolism, and metastasis can be described in terms of two transitions: hypoxia leads to changes in metabolism (mainly through the HIF-1α pathway) and changes in metabolism lead to changes in metastatic behavior. In many contexts, cancer can be thought of as a car with no brakes and full acceleration. Tumor cells can use the main mechanisms of metabolism, glycolysis and oxidative phosphorylation (OXPHOS), at maximum efficiency under different tumor microenvironments (TME) to create this "full acceleration" effect for growth and proliferation. Under normal conditions, normal cells use oxidative phosphorylation in the mitochondria to produce most adenosine triphosphate (ATP), while cancer cells turn to glycolysis for ATP production, resulting in a decreased dependency on oxygen. This switch to glycolysis under anaerobic conditions is a well-known phenomenon called the Warburg effect[27].

This switch in metabolism is chiefly brought about by a hypoxic change to the TME. Under hypoxia, the HIF-1α transcription factor facilitates the upregulation of genes such as GLUT-1 and PDK, which in turn increase glucose uptake[28,29]. This change to a more glycolytic metabolic profile allows the tumor cell to become less dependent on oxygen for energy. As a result of increased angiogenesis due to HIF-1α stabilization, blood vessels become more permeable to cells, allowing for metastasis[14,30]. A 2018 study revealed three types of breast cancer cells lines were 1.5-3 times more likely to engage in extravasation under hypoxic stress[31]. In most cases, regardless of tumor phenotype, hypoxia within the TME leads to less favorable outcomes for the patient.

Objectives

It is well known that tumor cells are often hypoxic and nutritionally deficient in vivo, so this project attempts to simulate these conditions in vitro[32]. The goal of project is to develop a clear understanding of how ROS signaling, and ultimately HIF-1α expression, are affected by intermittent and chronic hypoxia environments within murine breast cancer tumor cells of high and low metastatic potential. Based on previous research, the results should indicate that ROS generation will be greatly increased under intermittent hypoxia compared to chronic hypoxia, under nutrient-poor conditions compared to low-nutrient conditions, and for both metastatic cells compared to nonmetastatic cells. There should also be an initial increase in ROS production from both the metastatic and nonmetastatic cell lines, followed by a decrease in ROS production in the 4T1 cells, due to increased survivability.

Experimental Methods

Pilot Experiment – Cells were plated at a density of 150k cells per 35 mm^2 dish, treated with menadione sodium bisulfite at a concentration of 30 μM dissolved in distilled water, and incubated for 1 hour at 37℃. Menadione, also known as Vitamin K3, is a polycyclic aromatic ketone that induces the production of ROS within cells via redox cycling. Low concentrations of menadione mimic the oxidative stress experienced by tumors *in vivo*. After the first incubation period, CellROX Deep Red (Invitrogen, Carlsbad, California) was added to each plate at a final concentration of 5 μM. Cells were imaged according to protocol outline in ROS imaging section.

Cell Culture – The 4T1 (metastatic) and 67NR (nonmetastatic) murine breast cancer cells were cultured using Dulbecco's Modified Eagle's Medium (DMEM)

supplemented with 10%(v/v) of Fetal Bovine Serum (FBS), 2 mM L-Glutamine, 1% (v/v) nonessential amino acids, and 1%(v/v) penicillin-streptomycin in a humidified incubator that was set to 5% CO_2 and 37℃. Cells were passaged when 80% confluent and experimented on within the first 4 passages.

Hypoxia Exposure Procedure – A dual gas controller (Oxycycler C42, Biospherix, Parish, NY) connected to a modular sub-chamber was used to control oxygen, nitrogen, and carbon dioxide levels. The modular sub-chamber, which housed the cell plates, was placed inside an incubator. For chronic hypoxia, the gas controller was set to a constant level of 1% O_2 and 5% CO_2 for different lengths of time for each experiment. For intermittent hypoxia, the controller was set to cycle between 1% O_2 and 8% O_2 , with each hypoxia/normoxia period lasting 30 minutes. Total hypoxic exposure time for the intermittent physiological experiment matched that of the chronic physiological hypoxia experiment (Fig. 3).

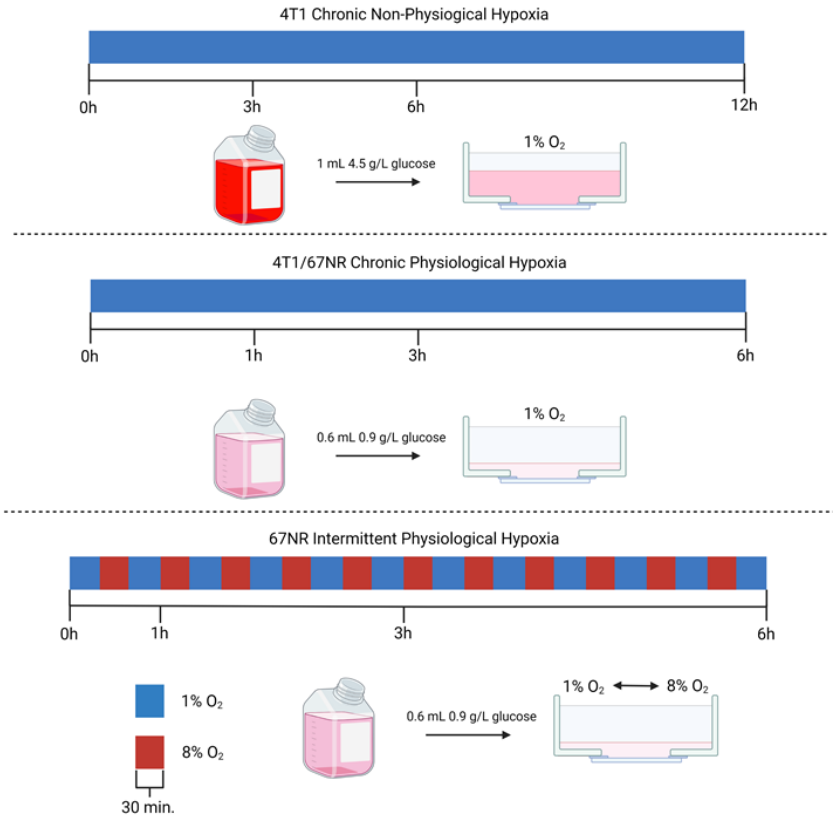

Figure 3. Graphic depicting experimental conditions

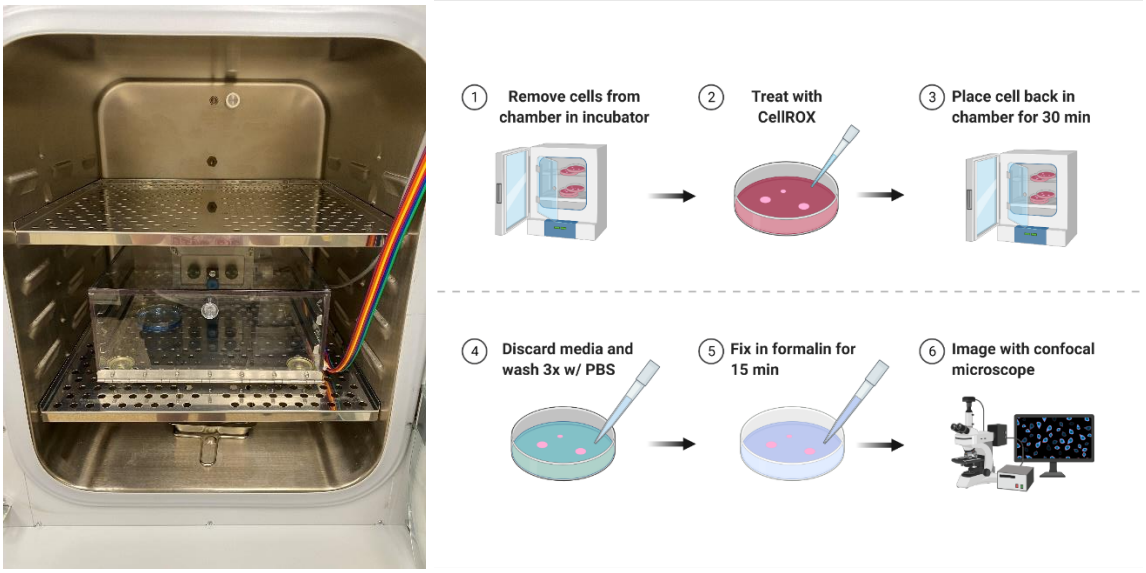

Figure 4. Picture of hypoxia chamber setup (left). Diagram of CellROX treatment protocol (right).

ROS Imaging – The cells were treated with the CellROX Deep Red (Invitrogen, Carlsbad, California) oxidative stress probe at a concentration of 5 μM and incubated for 30 minutes at 37℃ at each time point. After incubation, the cells were subsequently fixed with formalin (3.7% formaldehyde) for 15 minutes and imaged with a Fluoview FV10i confocal laser scanning biological microscope (Olympus, Tokyo, Japan) at 640/665 nm excitation/emission wavelengths (Fig. 4). For each pilot experiment, 3 plates were imaged per group. For each hypoxia experiment, 3 plates were imaged at each timepoint. However, two plates were removed from the baseline group in the 67NR chronic hypoxia experiment due to low cell density, and one plate was removed from the 4T1 physiological chronic hypoxia experiment due to photobleaching. Plates were imaged at 3 ROIs at 60x for the pilot experiments and 10x using a 3x3 grid for the hypoxia experiments. All images were taken at 49.6% sensitivity and 60% laser power.

Non-physiological (Non-Phys) vs. Physiological (Phys) condition – In the non-physiological condition, the cells (150k/confocal plate) were supplied with 1mL of the media recipe mentioned in the cell culture section. In the physiological condition, the cell culture media was diluted 1:5 using DI water to simulate the low-nutrition environment typically found in hypoxic areas of a tumor and normoxia was defined as 8% O2. Additionally, taking the oxygen diffusion limit into consideration, the volume of media in each plate was minimized to allow for maximal gas diffusion into the cells. It was determined that 600 μL of diluted media was the minimal volume of media that could be used without drying up.

Image Analysis – Images collected from the Fluoview FV10i confocal microscope were analyzed according to pixel-by-pixel fluorescent intensity from the CellROX Deep Red probe. Each image, in the TIFF format, was loaded into MATLAB, normalized to the maximum possible intensity value, and given a threshold value based on Otsu's method. Every pixel below the threshold value was labeled as 'dark' and every pixel greater than 0.9 was labeled as 'saturated'. The number of dark and saturated pixels were input into a function used to "stretch" the histogram by setting dark pixels to 0 and saturated pixels to 1. Next, the histogram was created using 2^{16} bins for optimal resolution. After creating histograms for each image, all histograms for each group were combined into one histogram using a cumulative sum of counts. The count number was then normalized to the total number of pixels less than 1 and greater than 0. Gaussian fits were generated using the Curve Fitter Tool in MATLAB.

Results

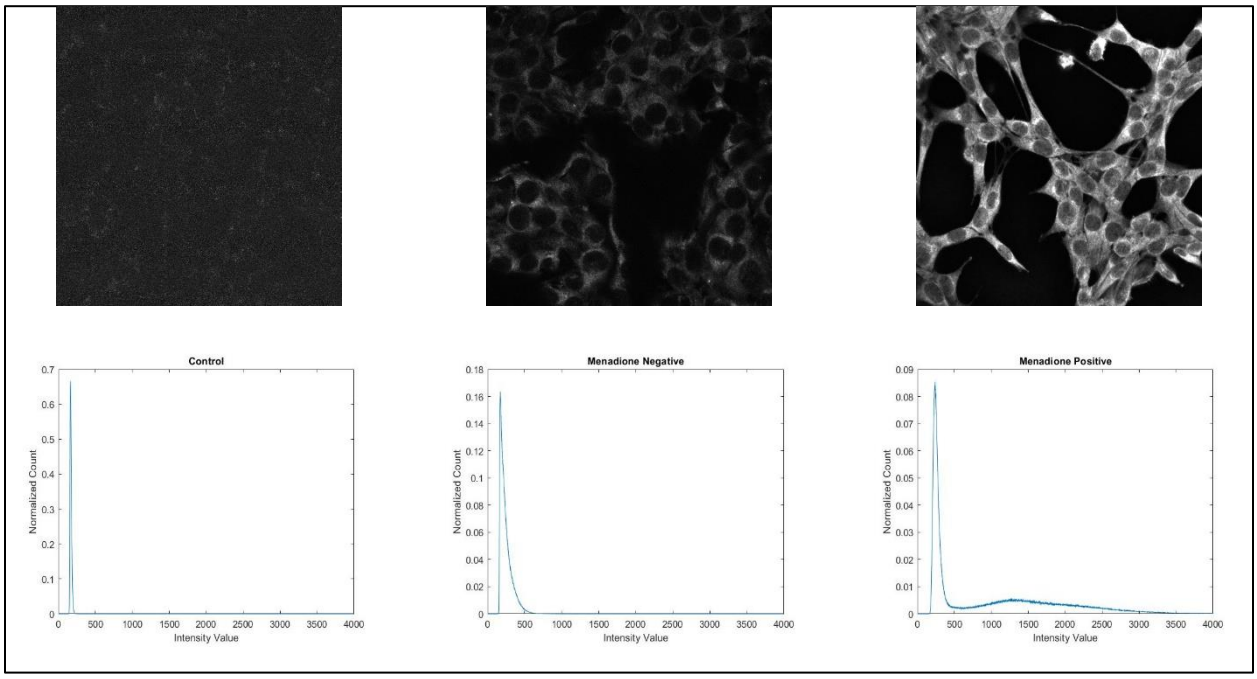

Figure 5. Each image of 67NR cells is represented by the histogram below it. From left to right, the images show cell in the control group, menadione negative group, and menadione positive group. As shown in each image-histogram pair, a darker image corresponds to a more left-shifted peak in the histogram.

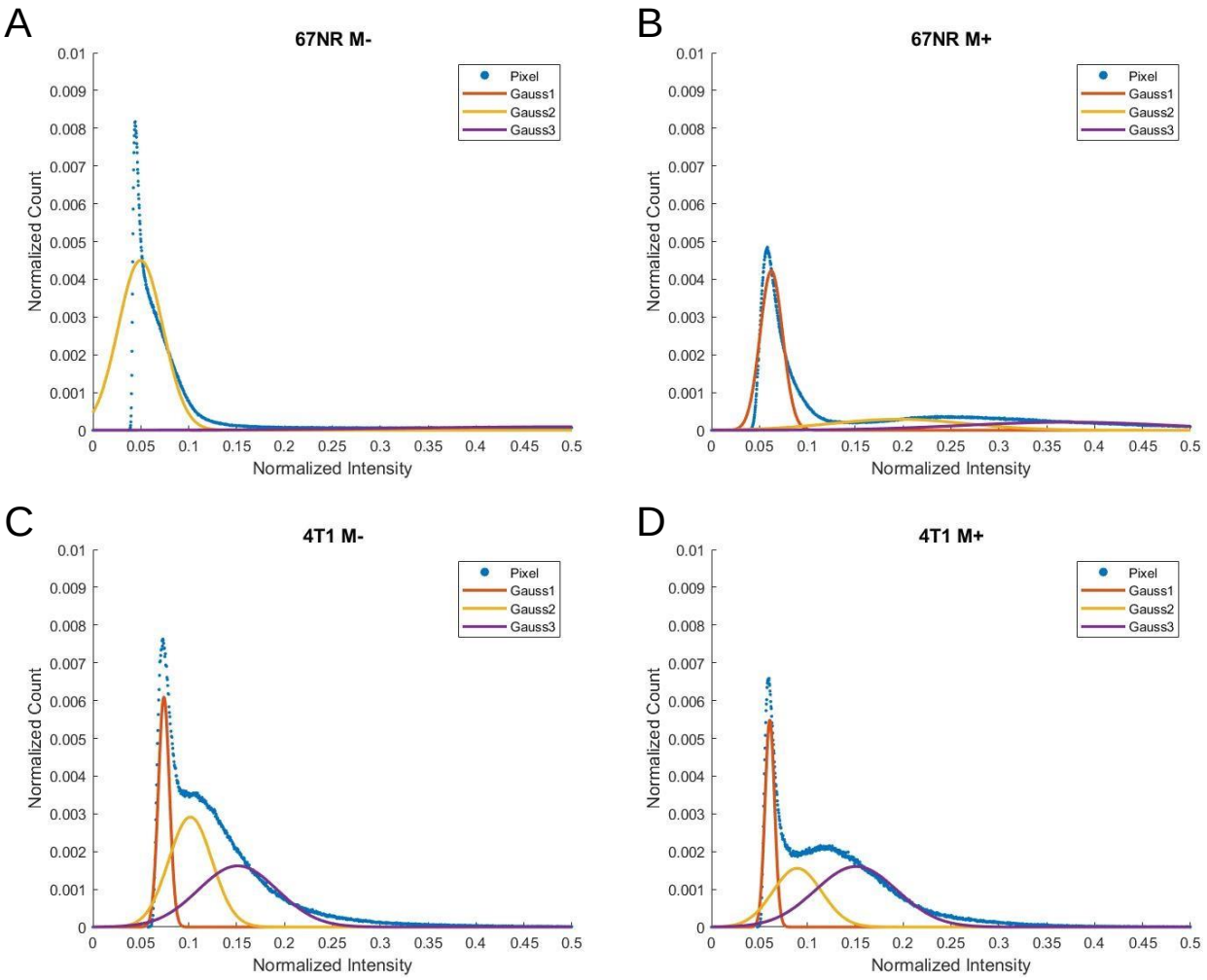

Figure 6. Histograms displaying intensity normalized to max intensity value (x-axis) and counts normalized to total number of counts in the sample (y-axis). Comparing the left and right graphs reveals differences in response between M- and M+ groups. Comparing the top and bottom graphs reveals differences in response between cell lines.

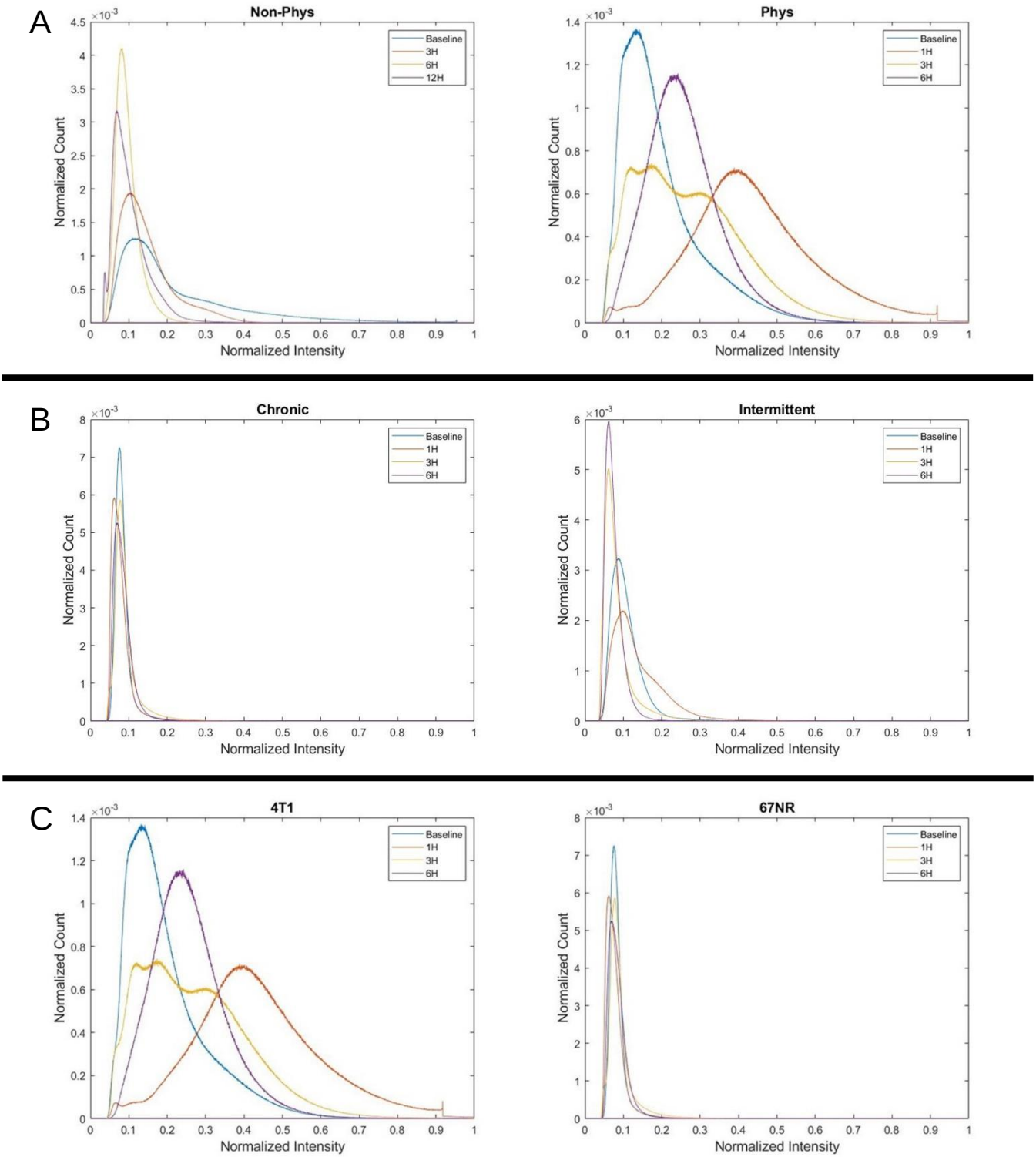

Figure 7. Each of the histograms in this figure are cumulative sums of each group normalized to the max intensity value (x-axis) and the total number of pixels for each group. Every pair of plots shows how the ROS generation profiles change over time under the different conditions: A) physiological vs. non-physiological, B) chronic vs. intermittent Hypoxia, and C) 67NR vs. 4T1 cell lines under chronic hypoxia.

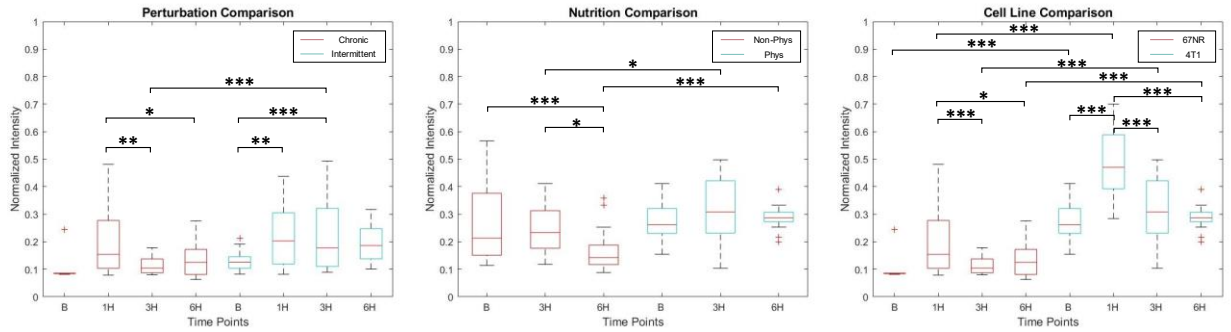

Figure 8. Distribution plots comparing intensity distributions for each experimental condition. The boxes in red on the left of each graph represent one experimental condition, while the boxes on the left in blue represent the other experimental condition. Left) One instance of significant difference was detected between groups and four were detected within groups. Middle) Two instances of significant difference were detected between groups and two were detected within the non-phys group. Note, only similar time points were statistically compared for the nutrition condition. Right) Four instances of significant difference were detected between groups and five were detected within groups. (*p<0.05,**p<0.01,***p<0.001, Tukey Post-Hoc Test).

4T1 and 67NR Cells Respond Differently to Redox Cycling

Menadione, the chemical used to treat the experimental group in the pilot experiments, induces oxidative stress via futile redox cycling. Futile redox cycling creates ROS in both the mitochondria and cytosol, prompting multiple redundant cell death pathways to activate if oxidative destruction of DNA is severe. However, apoptosis is not required for ROS-dependent mechanisms to come into effect[33]. Figure 5 depicts how the histograms quantify CellROX fluorescent intensity in each of the images taken with the confocal microscope. An image with no fluorescence will appear as a narrow peak, an image with low fluorescence will appear as a slightly broader peak, and an image with high fluorescence will appear as a second broad peak shifted to the right. In Figure 6, the fluorescence profiles resulting from menadione exposure can be seen for 4T1 and 67NR cells. The top and bottom rows of Figure 6 indicate 67NR cells exhibit increased sensitivity to oxidative stress resulting from menadione

exposure compared to 4T1 cells. Within Figure 6a, the Gauss2 fit is clearly visible, while the Gauss1 and Gauss3 fits are flat. This likely indicates most fluorescence is either background or low-level signal. In contrast, the menadione-positive 67NR cells exhibit increased fluorescent intensity, with Gauss2 and Gauss3 showing peaks at about 0.2 and 0.4, respectively.

The 4T1 cells, however, appear to react much differently to menadione-induced oxidative stress. The histograms in the bottom row of Figure 6 have little difference between them, with each Gaussian fit lying in approximately the same position in both figures. Since Gauss3 is strongly pronounced and right shifted compared to the other Gauss fits in both figures, it is reasonable to conclude that the 4T1 cells maintain a notably higher level of ROS than the 67NR cells in the unstressed and stressed oxidative states.

Physiological Conditions Result in Increased ROS Production

Within Figure 7a, each of the histograms corresponding to each timepoint fall in approximately the same position, indicating the fluorescence profiles of a 4T1 cell population does not change much when provided with ample nutrition. However, the change between the time points trend towards a narrower distribution in the low signal region of the graph. Under the nutrient-limited condition (Fig 7b), the 4T1 cells undergo an intensely high level of ROS generation at the 1-hour time point, followed by a reduced, but still relatively high level of ROS generation at the 3- and 6-hour time points. Interestingly, the histogram for the 3-hour timepoint appears to have three peaks at about 0.12, 0.18, and 0.30. At these points on the x-axis, there is the most overlap between the histograms of the individual images, but the peaks of the corresponding

individual histograms are at 0.11, 0.29, and 0.34. This indicates the variance between the individual histograms may be high compared to the other groups.

When comparing the non-physiological and physiological conditions, the physiological conditions induce a much stronger ROS generation profile within the 4T1 cells, as evidenced by broader, more right-shifted peaks in Figure 7. The box and whisker plot for the nutrition condition in Figure 8 indicates there was a significant difference between the two groups at the 3- and 6-hour time points.

67NR and 4T1 Cells Exhibit Differential ROS Profiles under Hypoxic Conditions

The 67NR hypoxia experiments were designed to compare hypoxia exposure times. Compared to the chronic hypoxia experiment, the intermittent hypoxia experiment shows a slight initial increase in ROS generation before declining to levels seen in chronic hypoxia. The fluorescence profiles of each time group within the chronic hypoxia group are extremely similar, indicating little to no change in ROS generation. Under the intermittent hypoxia condition, there is a slight initial increase at the 1-hour time point, but every time point afterward shows intensity levels below baseline. The perturbation comparison in Figure 8 reveals statistically significant differences between oxygenation conditions only at the 3-hour time point, in which there is an increase under intermittent hypoxia.

When comparing both cell types across chronic hypoxia conditions, 4T1 cells have greatly increased fluorescence at all time points compared to 67NR cells. This contrast is most evident when comparing between histograms in Figure 7c. Additionally, the right-most plot in Figure 8 shows a high number of statistical differences between the two cell lines. The largest difference appears to occur at the 1-hour time point

between the groups, with the 4T1 cells displaying about a 3.5-fold increase in ROS generation. While the fluorescence profiles of the 67NR cells show almost no change over time, the fluorescence profiles of the 4T1 cells show significant change over time within the chronic hypoxia condition.

Discussion and Future Works

ROS Control Mechanisms

The pilot experiment was primarily designed to test the ability of the CellROX Deep Red probe to detect excess ROS generation within the cells, but it also has the purpose of evaluating the effectiveness of ROS scavenging between the two cell lines. The results in Figure 6 suggest the 4T1 cells are more efficient at maintaining constant low levels of ROS compared to the 67NR cells, which appear to allow more ROS to be produced with the addition of menadione. Because 4T1 cells are known to be highly metastatic, it is likely that the 4T1 cells possess certain ROS regulatory mechanisms to keep ROS levels sufficient to produce a HIF-1α response, and in turn, an increase in metastasis, but not so high as to become destructive to the cell. However, this study cannot conclusively prove this idea of ROS self-regulation without knocking out the cell's ability to regulate ROS and testing for metastases *in vivo*. One possible explanation of this "ROS-regulation" mechanism could lie in the interplay between HIF-1α and NRF2, a transcription factor that promotes antioxidant defense. In studies done on NRF2 thus far, there exists a rather complex relationship between HIF-1α and NRF2. In some colorectal cell lines, HIF-1α is shown to regulate NRF2, but silencing NRF2 expression results in reduced HIF-1α and VEGF expression[34,35].

Survivability vs. Metastatic Potential Trade-Off

In a sense, a lack of nutrients necessary for tumor growth would provide a reason for metastasis within a 4T1 tumor. As evidenced in the nutrition condition experiments (Figure 7a), there is an increase in ROS level when the cells are exposed to a more stressful environment in terms of glucose and amino acid supply. Under the non-physiological, high-nutrient condition, the cells start at the baseline with the highest level of fluorescence. From this point, fluorescence decreased slightly over time, directly correlating with a decrease in ROS levels as well (Figure 7a). This could indicate the cells are opting for a more "survival-based" mode that favors growth over survivability and growth over mobility. When the cells are more nutrient starved, ROS generation increases greatly over the first hour before returning to a lower, yet likely sufficiently high level of ROS generation to encourage metastasis. This would suggest a switch to a more "metastasis-based" mode. This idea of switching between metabolic states matches with the current understanding of metabolic plasticity, defined as the ability of more metastatic cells to switch between OXPHOS and glycolysis depending on metabolite availability[36]. In fact, it has been shown that 4T1 cells have to ability use OXPHOS efficiently during optimal growth conditions and reversibly switch between glycolysis and OXPHOS during transient hypoxia[37].

Within the hypoxia context, the 67NR cells exhibit a slightly increased ROS generation profile under intermittent hypoxia compared to chronic hypoxia. This increase can be explained by a simple increase in oxygen within the surrounding environment. With increased oxygen flux into the cells, more oxygen radicals will be produced. Even under intermittent hypoxia, the 67NR cells are still able to maintain a

relatively low level of ROS generation. A study performed on human triple-negative breast cancer cells revealed accumulation of HIF-1α under intermittent hypoxia led to decreased proliferation and increased migration [38]. Since 67NR cells are not triple-negative and nonmetastatic, it is possible that ROS are kept under tighter control because there is no value in their ability to promote metastasis. Under chronic hypoxia, the ROS generation profile does not appear to change much over time according to Figure 7a. Since 67NR cells are not known to be metastatic, it is possible these cells lack the mechanisms necessary to use ROS to encourage metastasis.

When comparing 4T1 and 67NR cells under the same experimental conditions, striking differences can be observed between the two. Figure 7c displays that 4T1 cells allow much higher levels of ROS generation than the 67NR cells. As mentioned in the previous section, it appears the concept of a growth-focused metabolism vs. a metastasis-focused metabolism holds and is exacerbated by hypoxia. In terms of both ROS fluctuation over time and average ROS levels over the course of the experiment, 4T1 cells clearly exhibit a higher tolerance, and perhaps even a preference, to higher ROS levels over their nonmetastatic 67NR counterparts. This observation provides compelling evidence that ROS can be considered a signaling molecule for metastasis. However, it is yet to be proven that elevated ROS levels are indeed a cause of increased metastatic potential rather than simply being a characteristic of metastatic cells.

Future Work

Although this study can provide one possible explanation for metabolic differences in 4T1 cells and 67NR cells, the mechanisms behind increased ROS

generation and ROS levels might be modulated within the cell can still be explored. Within the hypoxia context, this experimental setup did well to quantitatively measure ROS by obtaining the fluorescent signal of the molecular probe after fixation of the cells, but being able to gather ROS data in a live-cell experiment within a closed system will more closely resemble the hypoxic processes within the body. To accomplish this, future studies should consider growing organoids within a sealed microfluidic chip to ensure tighter control over oxygen and nutritional supply. If the cells can be imaged without exposure to ambient oxygen, the possibility of increase ROS due to increased oxygen supply can be ruled out, therefore increasing the probability of observing ROS generation resulting from downregulation of ROS scavengers.

Provided that increased levels of ROS generation within breast cancer tumors indicate an increase in metastatic potential, the implications of this concept have the potential revolutionize cancer prognosis. One promising method for noninvasive detection is autofluorescence multispectral imaging technique[39]. Other optical methods, such as diffuse reflectance spectroscopy and Raman spectroscopy, are also being developed to better characterize the heterogeneity of tumors noninvasively. These optical methods could be used in conjunction with exogenous agents to evaluate and reduce the impact of ROS on tumor metastasis.

Acknowledgements

We would like to thank Dr. Kyle Quinn for access to the confocal microscope. We would also like to thank Paola Monterroso-Diaz and Jesse Ivers for their assistance with data analysis.

References

1. Fidler IJ. The pathogenesis of cancer metastasis: the “seed and soil” hypothesis revisited. *Nature Reviews Cancer*. 2003;3(6):453-458. doi:10.1038/nrc1098

2. Turrens JF. Mitochondrial formation of reactive oxygen species. *Journal of Physiology*. 2003;552(2):335-344. doi:10.1113/jphysiol.2003.049478

3. Costa A, Scholer-Dahirel A, Mechta-Grigoriou F. The role of reactive oxygen species and metabolism on cancer cells and their microenvironment. *Seminars in Cancer Biology*. 2014;25:23-32. doi:10.1016/j.semcancer.2013.12.007

4. Halliwell B. Oxidative stress and neurodegeneration: where are we now? *J Neurochem*. 2006;97:1634-1658. doi:10.1111/j.1471-4159.2006.03907.x

5. Han D, Antunes F, Canali R, Rettori D, Cadenas E. Voltage-dependent anion channels control the release of the superoxide anion from mitochondria to cytosol. *Journal of Biological Chemistry*. 2003;278(8):5557-5563. doi:10.1074/jbc.M210269200

6. Kirtonia A, Sethi G, Garg M. The multifaceted role of reactive oxygen species in tumorigenesis. *Cellular and Molecular Life Sciences*. 2020;77(22):4459-4483. doi:10.1007/s00018-020-03536-5

7. Yazaki K, Matsuno Y, Yoshida K, et al. ROS-Nrf2 pathway mediates the development of TGF-β1-induced epithelial-mesenchymal transition through the activation of Notch signaling. *European Journal of Cell Biology*. 2021;100(7-8). doi:10.1016/j.ejcb.2021.151181

8. Li Q, Engelhardt JF. Interleukin-1β induction of NFκB is partially regulated by H2O2-mediated activation of NFκB-inducing kinase. *Journal of Biological Chemistry*. 2006;281(3):1495-1505. doi:10.1074/jbc.M511153200

9. Liao Z, Chua D, Tan NS. Reactive oxygen species: A volatile driver of field cancerization and metastasis. *Molecular Cancer*. 2019;18(1). doi:10.1186/s12943-019-0961-y

10. Cadet J, Wagner JR. DNA Base Damage by Reactive Oxygen Species, Oxidizing Agents, and UV Radiation. doi:10.1101/cshperspect.a012559

11. Kang MA, So EY, Simons AL, Spitz DR, Ouchi T. DNA damage induces reactive oxygen species generation through the H2AX-Nox1/Rac1 pathway. *Cell Death and Disease*. 2012;3:249. doi:10.1038/cddis.2011.134

12. Semenza GL. Targeting HIF-1 for cancer therapy. *Nature Reviews Cancer*. 2003;3(10):721-732. doi:10.1038/nrc1187

13. Lee JW, Eo Ng-H U I B Ae S, On Jeong JW, Im SEHEK, Im KYWOK. Hypoxia-inducible factor (HIF-1)α: its protein stability andbiological functions. *EXPERIMENTAL and MOLECULAR MEDICINE*. 2004;36(1):1-12.

14. Muz B, de la Puente P, Azab F, Azab AK. The role of hypoxia in cancer progression, angiogenesis, metastasis, and resistance to therapy. *Hypoxia*. Published online December 2015:83. doi:10.2147/hp.s93413

15. Chandel NS, McClintock DS, Feliciano CE, et al. Reactive oxygen species generated at mitochondrial Complex III stabilize hypoxia-inducible factor-1α during hypoxia: A mechanism of O2 sensing. *Journal of Biological Chemistry*. 2000;275(33):25130-25138. doi:10.1074/jbc.M001914200

16. Lee DE, Alhallak K, Jenkins S v., et al. A Radiosensitizing Inhibitor of HIF-1 alters the Optical Redox State of Human Lung Cancer Cells in Vitro. *Scientific Reports*. 2018;8(1). doi:10.1038/s41598-018-27262-y

17. Dewhirst MW, Cao Y, Moeller B. Cycling hypoxia and free radicals regulate angiogenesis and radiotherapy response. *Nature Reviews Cancer*. 2008;8(6):425-437. doi:10.1038/nrc2397

18. Vaupel P, Harrison L. Tumor Hypoxia: Causative Factors, Compensatory Mechanisms, and Cellular Response. *The Oncologist*. 2004;9(S5):4-9. doi:10.1634/theoncologist.9-90005-4

19. Chaplin DJ, TMJ, DRE, OPL, MAI. Evidence for intermittent radiobiological hypoxia in experimental tumour systems. *Biomed Biochim Acta*. 1989;48(2-3):S255-S259.

20. Wenger R, Kurtcuoglu V, Scholz C, Marti H, Hoogewijs D. Frequently asked questions in hypoxia research. *Hypoxia*. Published online September 2015:35. doi:10.2147/hp.s92198

21. Leichtweiss HP, Lübbers DW, Weiss Ch, Baumgärtl H, Reschke W. The oxygen supply of the rat kidney: Measurements of intrarenalpO2. *Pfülgers Archiv European Journal of Physiology*. 1969;309(4):328-349. doi:10.1007/BF00587756

22. Groebe K, Vaupel P. Evaluation of oxygen diffusion distances in human breast cancer xenografts using tumor-specific in vivo data: Role of various mechanisms in the development of tumor hypoxia. *International Journal of Radiation Oncology*Biology*Physics*. 1988;15(3):691-697. doi:10.1016/0360-3016(88)90313-6

23. Olive PL, Vikse C, Trotter MJ. Measurement of oxygen diffusion distance in tumor cubes using a fluorescent hypoxia probe. *International Journal of Radiation Oncology*Biology*Physics*. 1992;22(3):397-402. doi:10.1016/0360-3016(92)90840-E

24. Grimes DR, Kelly C, Bloch K, Partridge M. A method for estimating the oxygen consumption rate in multicellular tumour spheroids. doi:10.1098/rsif.2013.1124

25. Vaupel P, Mayer A, Höckel M. Strahlentherapie und Onkologie Impact of Hemoglobin Levels on Tumor Oxygenation: the Higher, the Better? *Strahlenther Onkol*. 2006;182(2):63-71. doi:10.1007/s00066-006-1543-7

26. Mckeown SR. Defining normoxia, physoxia and hypoxia in tumours-implications for treatment response. *Br J Radiol*. 2014;87. doi:10.1259/bjr.20130676

27. Warburg O. On the Origin of Cancer Cells. *Science (1979)*. 1956;123(3191):309-314. doi:10.1126/science.123.3191.309

28. Emami Nejad A, Najafgholian S, Rostami A, et al. The role of hypoxia in the tumor microenvironment and development of cancer stem cell: a novel approach to developing treatment. *Cancer Cell International*. 2021;21(1). doi:10.1186/s12935-020-01719-5

29. Colwell N, Larion M, Giles AJ, et al. Hypoxia in the glioblastoma microenvironment: Shaping the phenotype of cancer stem-like cells. *Neuro-Oncology*. 2017;19(7):887-896. doi:10.1093/neuonc/now258

30. Carmeliet P, Jain RK. Molecular mechanisms and clinical applications of angiogenesis. *Nature*. 2011;473(7347):298-307. doi:10.1038/nature10144

31. Song J, Miermont A, Lim CT, Kamm RD. A 3D microvascular network model to study the impact of hypoxia on the extravasation potential of breast cell lines. *Scientific Reports*. 2018;8(1). doi:10.1038/s41598-018-36381-5

32. Vaupel P, Kallinowski F, Okunieff P. Blood flow, oxygen and nutrient supply, and metabolic microenvironment of human tumors: a review. *Cancer Res*. 1989;49(23):6449-6465.

33. Loor G, Kondapalli J, Schriewer JM, Chandel NS, vanden Hoek TL, Schumacker PT. Menadione triggers cell death through ROS-dependent mechanisms involving PARP activation without requiring apoptosis. *Radic Biol Med*. 2010;49(12):1925-1936. doi:10.1016/j.freeradbiomed.2010.09.021

34. Tafani M, Sansone L, Limana F, et al. The Interplay of Reactive Oxygen Species, Hypoxia, Inflammation, and Sirtuins in Cancer Initiation and Progression. Published online 2016. doi:10.1155/2016/3907147

35. Kovac S, Angelova PR, Holmström KM, Zhang Y, Dinkova-Kostova AT, Abramov AY. Nrf2 regulates ROS production by mitochondria and NADPH oxidase. *Biochimica et Biophysica Acta (BBA) - General Subjects*. 2015;1850(4):794-801. doi:10.1016/j.bbagen.2014.11.021

36. Al-Masri M, Paliotti K, Tran R, et al. Architectural control of metabolic plasticity in epithelial cancer cells. doi:10.1038/s42003-021-01899-4

37. Simões R v., Serganova IS, Kruchevsky N, et al. Metabolic Plasticity of Metastatic Breast Cancer Cells: Adaptation to Changes in the Microenvironment. *Neoplasia (United States)*. 2015;17(8):671-684. doi:10.1016/j.neo.2015.08.005

38. Liu L, Liu W, Wang L, Zhu T, Zhong J, Xie N. Hypoxia-inducible factor 1 mediates intermittent hypoxia-induced migration of human breast cancer MDA-MB-231 cells. *Oncol Lett*. 2017;14(6):7715-7722. doi:10.3892/ol.2017.7223

39. Habibalahi A, Moghari MD, Campbell JM, et al. Non-invasive real-time imaging of reactive oxygen species (ROS) using auto-fluorescence multispectral imaging technique: A novel tool for redox biology. *Redox Biology*. 2020;34. doi:10.1016/j.redox.2020.101561